JOC The Journal of Organic Chemistry

Article

pubs.acs.org/joc

LR-HSQMBC: A Sensitive NMR Technique To Probe Very Long-Range Heteronuclear Coupling Pathways

R. Thomas Williamson,*[,†] Alexei V. Buevich,[‡] Gary E. Martin,[§] and Teodor Parella[∥]

[†]Discovery & Preclinical Sciences, Process & Analytical Chemistry, Structure Elucidation Group, Merck & Co. Inc., Rahway, New Jersey 07065, United States

[‡]Discovery & Preclinical Sciences Process & Analytical Chemistry Structure Elucidation Group, Merck & Co. Inc., Kenilworth, New Jersey 07033, United States

[§]Discovery & Preclinical Sciences Process & Analytical Chemistry Structure Elucidation Group, Merck & Co. Inc., Summit, New Jersey 07901, United States

[∥]Servei de Ressonància Magnètica Nuclear and Departament de Química, Universitat Autònoma de Barcelona, E-08193 Bellaterra, Barcelona, Spain

Supporting Information

ABSTRACT: HMBC is one of the most often used and vital NMR experiments for the structure elucidation of organic and inorganic molecules. We have developed a new, high sensitivity NMR pulse sequence that overcomes the typical $^{2,3}J_{CH}$ limitation of HMBC by extending the visualization of long-range correlation data to 4-, 5-, and even 6-bond long-range $^{n}J_{CH}$ heteronuclear couplings. This technique should prove to be an effective experiment to complement HMBC for probing the structure of proton-deficient molecules. The LR-HSQMBC NMR experiment can, in effect, extend the range of HMBC to provide data similar to that afforded by 1,*n*-ADEQUATE even in sample-limited situations. This is accomplished by optimizing responses for very small $^{n}J_{CH}$ coupings as opposed to relying on the markedly less sensitive detection of long-range coupled $^{13}C-^{13}C$ homonuclear pairs at natural abundance. DFT calculations were employed to determine whether the very long-range correlations observed for cervinomycin A_2 were reasonable on the basis of the calculated long-range couplings.

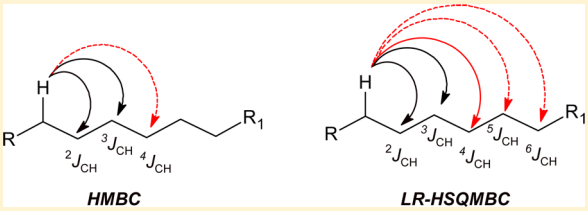

INTRODUCTION

Modern structure elucidation changed dramatically with the advent of two-dimensional NMR methods and has continued to evolve with the development of inverse-detected methods followed by the development of very high sensitivity small volume and cryogenic NMR probes. The sample size required for characterization by NMR methods correspondingly has been reduced with the technological advances, decreasing first to the milligram level and presently, with the use of 1.7 mm microcryoprobe capabilities, to a fraction of a micromole.

Several recent reviews have examined strategies utilized for the elucidation of natural product structures that can also be generally applied to any structure elucidation problem regardless of sample origin.[1,2] These approaches generally begin with the establishment of direct proton−carbon heteronuclear pairings using an experiment such as multiplicity-edited HSQC. Next, mapping out the proton−proton connectivity network is necessary. Classically, homonuclear proton−proton connectivities are mapped out using the COSY experiment. As molecular structures become progressively more complex and proton spectra become correspondingly more overlapped, experiments such as HSQC-TOCSY can be employed to disentangle and unequivocally assign proton spin coupling networks. Next, intervening quaternary carbons and/or heteroatoms must be positioned, and correlations across these positions established. Experiments such as NOESY and/or ROESY can be used to establish proton−proton connectivity through space via dipolar relaxation processes but require that there are sufficient protons located in key strategic locations in the molecule. Inevitably, increasing molecular complexity leads to situations in which correlations must be established in severely proton-deficient regions of a molecular structure, requiring an investigator to resort to long-range heteronuclear shift correlation methods. Prior to the advent of proton-detected NMR methods, experiments such as long-range HETCOR and FLOCK were used for this purpose with varying success.[3] In 1986, Bax and Summers reported the development of the HMBC experiment.[4] HMBC has become one of the most widely used NMR experiments and serves as one of the cornerstones of modern NMR-based structure elucidation strategies. The HMBC experiment has been the subject of numerous reviews and remains one of the most highly cited publications in the scientific literature.[5]

HMBC experiments, typically optimized in the range of 6−10 Hz, reliably provide access to predominantly $^{3}J_{CH}$

Received: February 11, 2014
Published: April 7, 2014

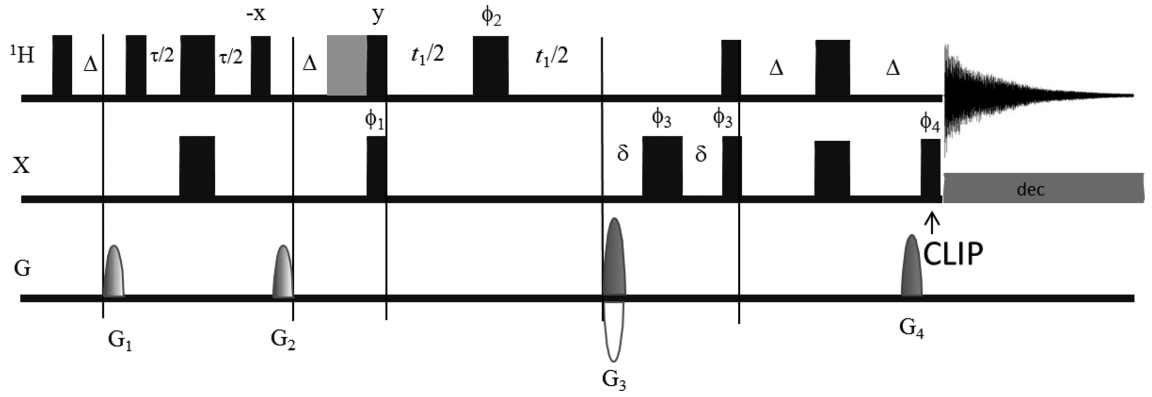

Figure 1. LR-HSQMBC pulse sequence. The pulse sequence begins with the standard $^{n}J_{CH}$ INEPT transfer of magnetization from ^{1}H to ^{13}C wherein a G-BIRD$_{R,X}$ segment efficiently suppresses $^{1}J_{CH}$ responses. The clean in-phase (CLIP) multiplets module at the end of the sequence helps to remove unwanted antiphase contributions from the desired in-phase multiplets.[13] The delay Δ is optimized for the long-range $^{n}J_{CH}$ coupling constant of interest ($^{n}J_{CH}$; 1/4 J_{CH}) and the delay τ is optimized for $^{1}J_{CH}$ (1/2 J_{CH}). All ^{13}C π pulses were adiabatic CHIRP pulses for broadband inversion and refocusing (see Supporting Information for details and phase cycling).

correlations with smaller $^{2}J_{CH}$ responses observed less often and $^{4}J_{CH}$ correlations visualized only intermittently. Occasionally, longer-range correlations are observed and have been the subject of two reviews by Araya-Maturana and co-workers.[6] Unfortunately, there is no way to reliably differentiate different coupling path lengths for HMBC correlations. This inherent limitation of the HMBC experiment prompted the development of the ^{2}J,^{3}J-HMBC experiment followed by the development of the H2BC experiment and variants.[7,8] While this latter group of pulse sequences works for the identification of protonated carbons adjacent to a given proton−carbon heteronuclide pair, these experiments do not work for adjacent nonprotonated carbons. This limitation on the ability to identify adjacent nonprotonated carbon resonances was circumvented by the development of the 1,1-ADEQUATE experiment in 1996 albeit at the price of significantly reduced sensitivity since the experiment employs a $^{1}J_{CC}$ homonuclear transfer.[9]

As molecular structures become progressively more proton-deficient, there is an increasing need to establish $^{4}J_{CH}$ and sometimes still longer range connectivities. The 1,*n*-ADEQUATE experiment provides this capability via predominantly $^{3}J_{CC}$ (equivalent to $^{4}J_{CH}$) correlations but again, the application of this experiment is limited by its sensitivity, virtually requiring access to small volume cryogenic NMR probe capabilities if the technique is to be applied in the low milligram range.[9] An alternative strategy is to optimize an HMBC experiment for a small long-range coupling in the range of 2−4 Hz. However, this optimization choice comes at the expense of considerable loss in sensitivity due to antiphase cancelation of responses and the longer duration of the delays necessitated by the targeted 2−4 Hz $^{n}J_{CH}$ correlations.

These developments have defined the need for an experiment with the capabilities of 1,*n*-ADEQUATE albeit with sensitivity more akin to that of an HMBC experiment. It was in this context that we began to explore the modification of the HSQMBC pulse sequence[10] and to adapt it for very long-range heteronuclear shift correlation. We now wish to report a new NMR experiment, LR-HSQMBC (long-range heteronuclear single quantum multiple bond correlation), which is complementary to the standard 8 Hz HMBC and affords comparably more "very long-range" $^{n}J_{CH}$ correlations (where n = 4−6), with higher sensitivity than can be realized with HMBC or D-HMBC when these experiments are optimized in the range of 2−4 Hz.[11] The pulse sequence itself is a simple refocused and decoupled modification of the G-BIRD$_{R,X}$-HSQMBC pulse sequence[10] optimized for the observation of very long-range correlations. An additional feature of the pulse sequence is the insertion of a 90° carbon pulse prior to acquisition to convert residual antiphase $2I_yS_z$ components to nonobservable $2I_yS_y$ multiple-quantum coherences. Accordingly, the experiment leads to predominantly in-phase multiplets that evolve according to $I_x \sin^2(\pi^{n}J_{CH}\Delta')$, and the intensity of the visualized correlations will present a dependence proportional to $k[\sin^2(\pi^{n}J_{CH}\Delta')]$, where k is a function described by $\cos(\pi J(H_x - H_y)\Delta')$. Therefore, a different delay optimization can be useful in the event that an expected correlation is missing (see Supporting Information). The pulse sequence schematic is shown in Figure 1. Alternatively, an approach employing homonuclear selective excitation of uncoupled ^{1}H−^{1}H pairs such as the CLIP-HSQMBC[12a] or EXSIDE[12b] could alleviate this problem.

Refocusing the desired $^{n}J_{CH}$ magnetization after the t_1 evolution time provides two advantages. First, it generates in-phase $^{n}J_{CH}$ correlations which avoid the antiphase cancelation of responses with very small coupling constants. This phenomenon is encountered with the standard HMBC and HSQMBC experiments and is exacerbated with decreasing digitization in the F_2 dimension. It can be shown that for small scalar coupling constants, in-phase (IP) cross-peaks are always larger than antiphase (AP) and the IP/AP ratio can quickly grow to ≫100 as the $^{n}J_{CH}$ coupling approaches values of 0.1−0.2 Hz (see Supporting Information for a more detailed description). For small coupling constants, this contribution to the difference between in-phase and antiphase cross peak intensities is overwhelmingly lager than any effects from the magnetization transfer. While LR-HSQMBC may not have greater sensitivity than an 8 Hz optimized HMBC, it does have greater sensitivity when both are optimized for 2 Hz due to the cancellation due to the antiphase nature of some long-range correlations when the data are magnitude calculated. Second, refocusing of the heteronuclear coupling allows the application of ^{13}C decoupling during the acquisition time. This operation collapses the heteronuclear coupling of the response and partially recovers some of the S/N lost as a result of relaxation processes encountered during the long duration of the delays

dx.doi.org/10.1021/jo500333u | J. Org. Chem. 2014, 79, 3887−3894

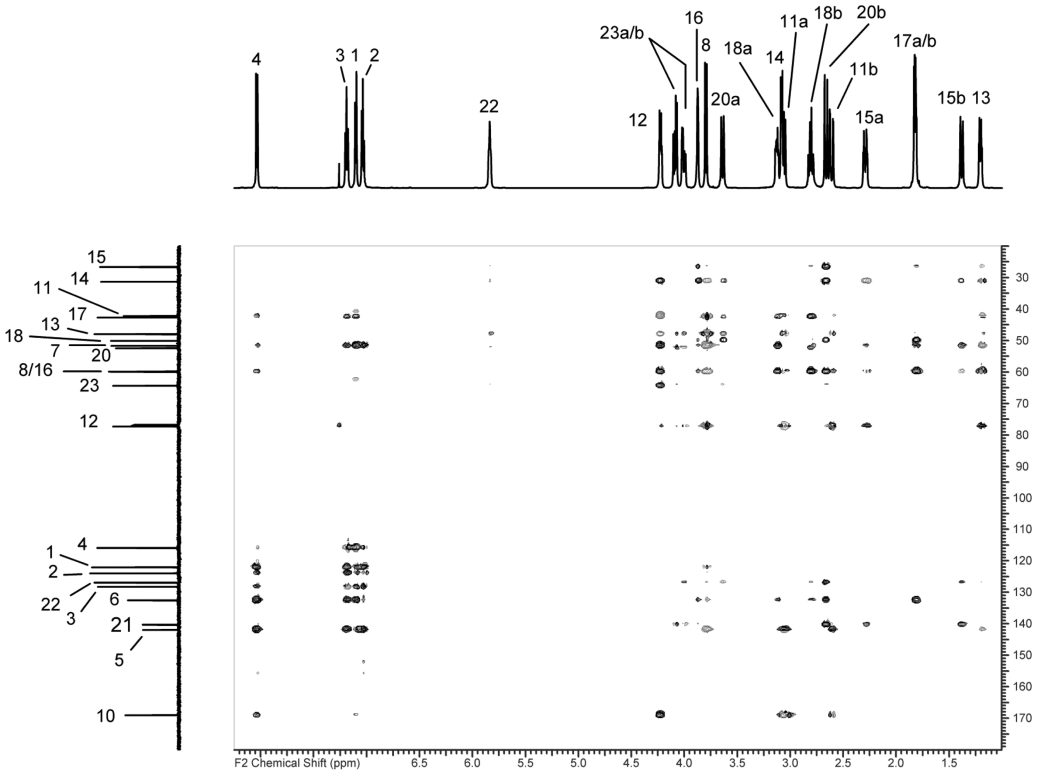

Figure 2. LR-HSQMBC spectrum of strychnine optimized for $^{n}J_{CH}$ = 2 Hz. The data were acquired using a 4.9 mg sample of strychnine (**1**) (10.5 μmol) dissolved in 40 μL of $CDCl_3$ as 4096 × 512 points with 32 transients accumulated per t_1 increment. The $^{1}J_{CH}$ delay was optimized for 145 Hz. A delay of 1.5 s was employed between transients, giving an overall acquisition time of 10 h 45 m. It should be noted, however, that data containing all of the correlations summarized in Table 1 were acquired for this sample in as little as 2 h 42 m with excellent signal-to-noise (see Supporting Information).

optimized for detection of very small $^{n}J_{CH}$ couplings. Selection of the delay leading to the smallest practical observable coupling constant should be made on the basis of an estimation of the T_2 losses for the molecule of interest. However, as shown in this report, even molecules as large as cervinomycin A_2[20] (527 Da) can provide exceptional data on submilligram samples. Finally, it should be noted that the information density of LR-HSQMBC due to the large number of detected $^{n}J_{CH}$ correlations is generally too high to be used directly without "filtering" of shorter range correlations that would come from HMBC.

RESULTS AND DISCUSSION

Strychnine. As a first example, we utilized strychnine (**1**) as a model compound to evaluate the performance of the LR-HSQMBC (Figure 2). Strychnine makes for an excellent test case since it is readily available and has been used as a standard in a plethora of NMR studies,[14] most of the heteronuclear couplings 2 Hz or larger are known,[15] and it has been shown previously to be amenable to accurate DFT calculations of scalar coupling constants.[15] To compare the effectiveness of this sequence for probing long and very long-range $^{n}J_{CH}$ connectivities, we acquired a baseline HMBC data set optimized for a standard 8 Hz $^{n}J_{CH}$ coupling, an HMBC adjusted for 2 Hz, and a decoupled HMBC (D-HMBC) also tuned to 2 Hz. The D-HMBC developed by Furihata and Seto is analogous to the LR-HSQMBC in that it is a refocused version of the standard HMBC experiment.[11]

As can be seen by the results in Table 1, the LR-HSQMBC provided a total of 68 very long-range correlations that reached

Table 1. Comparison of Responses in the LR-HSQMBC, D-HMBC, and HMBC Experiments[a]

expt	$^{2}J_{CH}$	$^{3}J_{CH}$	$^{4}J_{CH}$	$^{5}J_{CH}$	$^{6}J_{CH}$	total $>^{3}J_{CH}$	total
LR-HSQMBC 2 Hz	33	59	55	11	2	68	160
D-HMBC 2 Hz	29	43	34	8	2	44	115
HMBC 2 Hz	34	54	43	10	1	54	142
HMBC 8 Hz	35	53	36	4	1	41	129

[a]The 2 Hz LR-HSQMBC experiment affords 24.1% more $^{4}J_{CH}$ correlations, a 10% increase in $^{5}J_{CH}$ correlations, and a 100% increase in the number of $^{6}J_{CH}$ correlations relative to the next most efficient 2 Hz optimized HMBC experiment.

further than 3 bonds ($>^{3}J_{CH}$). There were 14 more very long-range responses compared with the 2 Hz HMBC, and 24 more very long-range responses than were observed in the D-HMBC data. It should also be noted that the LR-HSQMBC also revealed the largest total number of $^{n}J_{CH}$ correlations out of all experiments tested with a total of 160 $^{n}J_{CH}$ correlations.

In an effort to better understand the origin of the long-range and very long-range $^{n}J_{CH}$ couplings, we embarked on a detailed DFT study of strychnine (**1**). High accuracy was previously shown using the B3LYP functional and the 6-311+G(d,p) basis set in reproducing the $^{1}J_{CC}$ coupling constants.[16a] Specifically, the Fermi contacts (FC) were calculated on an uncontracted basis set with tighter polarization functions for the s and d orbitals.[17] To confirm that DFT calculations have a high accuracy of reproducing long-range and very long-range proton−carbon $^{n}J_{CH}$ couplings, we have compared them with known experimental values from several different groups including our own.[15] It appears that among different

dx.doi.org/10.1021/jo500333u | J. Org. Chem. 2014, 79, 3887−3894

approaches to measure long-range proton−carbon couplings, the IPAP-HSQC-TOCSY experiment[15] afforded the highest accuracy and sign determination of the couplings constants. As seen in Figure 3, the correlation between experimental IPAP-HSQC-TOCSY and DFT calculated $^{n}J_{CH}$ are nearly perfect, thus confirming a high accuracy of DFT calculations and assuring that they can also give reliable estimations of longer range couplings as well. The complete set of all calculated $^{n}J_{CH}$ couplings can be found in the Supporting Information.

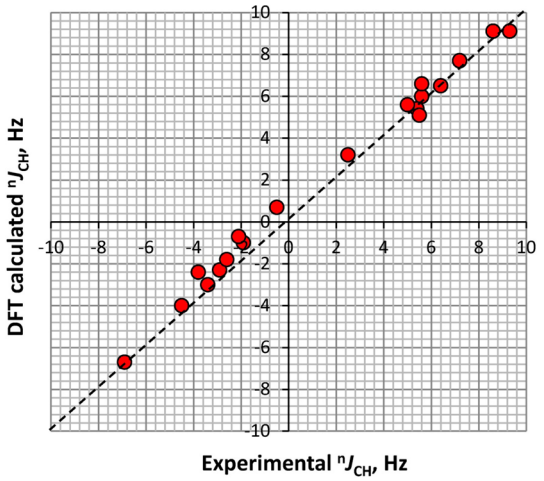

Figure 3. Correlation plot of experimental and DFT calculated $^{n}J_{CH}$ couplings. Experimental couplings were measured with the IPAP-HSQC-TOCSY pulse sequence,[15] and DFT calculations were performed at the B3LYP/6-311+G(d,p) level of theory as previously described for strychnine (**1**).[16a]

Among the long-range correlations noted in the LR-HSQMBC NMR data (Scheme 1), 22 were calculated to arise from $^{n}J_{CH}$ couplings ≤1.0 Hz and would not be expected to appear in any non-refocused experimental variant like a standard HMBC or HSQMBC spectrum due to antiphase cancellation of the relevant cross peaks. In fact, this is exactly what was observed in the LR-HSQMBC data in that all of the additional peaks visualized in the LR-HSQMBC data arise from these very small heteronuclear couplings (see Supporting Information for detailed table showing all calculated coupling constants and associated LR-HSQMBC correlations).

Scheme 1. LR-HSQMBC $^{n}J_{CH}$ Correlations of Strychnine (1) Calculated to Be Less than 0.2 Hz[a]

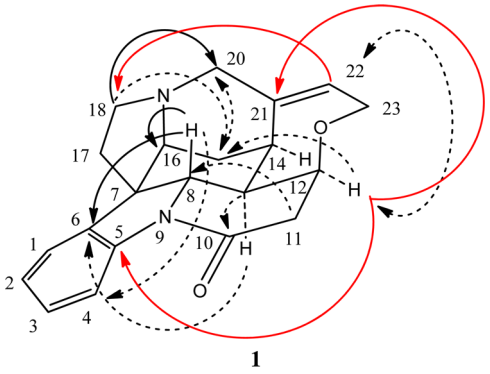

[a]Solid black arrows = $^{3}J_{CH}$; dashed black arrows = $^{4}J_{CH}$; solid red arrows = $^{5}J_{CH}$. Double-headed arrows denote mutually long-range coupled protonated carbon pairs. Quite likely, the large number of very long-range ($>^{3}J_{CH}$) heteronuclear couplings observed for strychnine is facilitated by the rigid structure of the molecule in everything other than the tetrahydropyrrole moiety.[16b,c].

Comparison of Strychnine LR-HSQMBC and Dual-Optimized Inverted $^{1}J_{CC}$ 1,*n*-ADEQUATE Data. As mentioned previously, our primary goal was to develop an experiment with information content comparable to that of the 1,*n*-ADEQUATE but with enhanced sensitivity via the $^{n}J_{CH}$ correlation pathway that does not rely on long-range coupled $^{13}C-^{13}C$ pairs. To explore this concept and prepare a starting point for comparison, we acquired a dual optimization inverted $^{1}J_{CC}$ 1,*n*-ADEQUATE spectrum optimized for $^{1}J_{CC}/^{n}J_{CC}$ couplings of 57/9.5 and 64/8 Hz for the long-range $^{13}C-^{13}C$ correlations.[9e] The dual-optimized inverted $^{1}J_{CC}$ 1,*n*-ADEQUATE spectrum with excellent signal-to-noise was acquired in 24 h 22 m. In total, there were 123 ADEQUATE correlations representing the equivalent information content of $^{2}J_{CH}$, $^{3}J_{CH}$, and $^{4}J_{CH}$ responses in the LR-HSQMBC and HMBC experiments. In comparison, 29 of the ADEQUATE correlations were missing in the LR-HSQMBC data (23.6%), but an additional 62 new correlations (50.4%) not observed in the inverted $^{1}J_{CC}$ 1,*n*-ADEQUATE data were visualized in the LR-HSQMBC experiment (see Supporting Information). This cumulative increase in long-range H−C connectivity information in the LR-HSQMBC data came with the commensurate advantage that the data could be acquired in less than 1/10 of the time required to acquire the 1,*n*-ADEQUATE spectrum and with far superior F_1-resolution. Moreover, it should also be noted that the greater sensitivity of the LR-HSQMBC experiment facilitates the application of the experiment in limited sample situations when it would not be feasible to undertake the acquisition of any type of ADEQUATE spectrum. While drawing comparisons, the sole negative attribute of the LR-HSQMBC experiment relative to dual-optimization inverted $^{1}J_{CC}$ 1,*n*-ADEQUATE is that the former does not allow the unequivocal differentiation of $^{1}J_{CC}$ from $^{n}J_{CC}$ ($^{2}J_{CH}$ vs $^{n}J_{CH}$ where $n \geq 3$) afforded by the latter experiment. However, given the significantly greater sensitivity of the LR-HSQMBC experiment, this trade-off should be acceptable in most situations.

Cervinomycin A_2. As a second example aimed at representing a more challenging and realistic structure problem, we prepared a sample of ∼400 μg of cervinomycin A_2 (**2**) (Apollo Scientific, Inc., Stockport, Cheshire SK6 2QR, U.K.). This novel xanthone antibiotic, which demonstrated potent inhibition of anaerobic and mycoplasmal growth, was first isolated by Ōmura and co-workers in 1982.[18] The challenging and proton-sparse structure with a Crews rule[19] ratio of <2 was eventually elucidated via a combination of chemical interconversion, synthesis of chemical derivatives, and detailed NMR studies of each.[20] The NMR investigations incorporated a battery of standard 1D and 2D ^{13}C-detected heteronuclear correlation experiments including HETCOR[21] and long-range selective decoupling experiments (LSPD).[22] These studies were facilitated in the original work by the ready availability of extremely soluble and stable cervinomycin A_2 analogues, specifically *O*-methylcervinomycin A_2 and *C*,*O*-dimethylcervinomycin A_2.[20] The production and analysis of *C*,*O*-diacetylcervinomycin A_2 and monoacetylcervinomycin A_2 also provided additional support for the proposed structure of cervinomycin A_2.[20] Finally, additional evidence was garnered through correlation of X-ray results from a series of related

dx.doi.org/10.1021/jo500333u | J. Org. Chem. 2014, 79, 3887−3894

compounds, namely, lysolipin,[23] albofungin and chloroalbofungin,[24] and LL-D42067 α and β.[25]

Cervinomycin A_2 represents an extremely proton-deficient molecule with large expanses of nonprotonated carbons between proton "handles". This description falls well within the definition of the Crews rule.[19] In addition, the limited sample quantity coupled with limited solubility even in deuterochloroform thwarted all attempts at the acquisition of 1,*n*- or even 1,1-ADEQUATE data in realistic time periods. We show here that with the aid of LR-HSQMBC data, the original structure can be elucidated and all ^{1}H and ^{13}C atoms assigned from NMR data and molecular formula alone without the need for any chemical degradation or derivatization.

After ^{1}H and ^{13}C assignment of all protonated carbons using a standard multiplicity edited-HSQC experiment, we embarked on a study utilizing HMBC and LR-HSQMBC experiments to examine whether we could cover the vast expanses of molecular functionality between the aromatic proton handles using the new pulse sequence in conjunction with standard HMBC data. As can be seen in Figure 4 and Scheme 2 below, there were 9

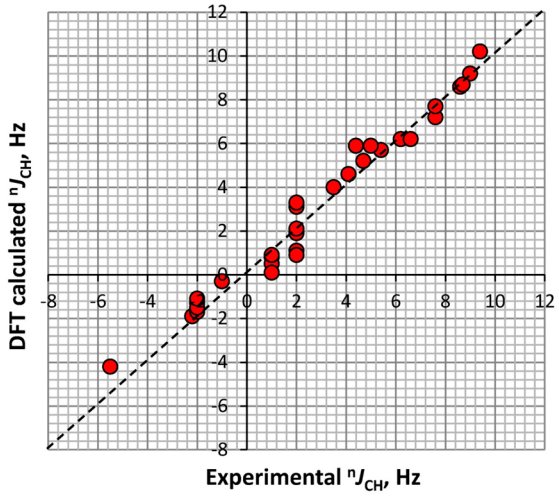

Figure 4. Correlation plot of experimental and DFT calculated $^nJ_{CH}$ couplings in cervinomycin A_2 (**2**). Experimental couplings were measured with CLIP-HSQMBC pulse sequence,[26] and DFT calculations were performed at the B3LYP/6-311+G(d,p) level of theory as previously described for strychnine (**1**).[16]

key very long-range $^4J_{CH}$ correlations visualized in the 4 Hz LR-HSQMBC compared to 8 such responses in the 4 Hz HMBC data, whereas the 2 Hz optimized LR-HSQMBC spectrum afforded 22 $^4J_{CH}$ correlations (Scheme 2). The LR-HSQMBC experiments also offered greater numbers of $^5J_{CH}$ correlations, and in the case of the 2 Hz optimized LR-HSQMBC experiment, 1 $^6J_{CH}$ correlation was observed. The calculated coupling constants for these correlations ranged from 0.45 to 1.28 Hz (in absolute values). As in the case of strychnine (**1**), couplings for cervinomycin A_2 (**2**) were calculated by DFT methods at the B3LYP/6-311+G(d,p) level of theory for the lowest energy conformation optimized at the B3LYP/6-31G(d) level of theory. To substantiate these calculated $^nJ_{CH}$ coupling constants, we utilized the CLIP-HSQMBC experiments[12a] to measure as many actual $^nJ_{CH}$ values as possible. As can be seen in Figure 4, the experimental values agreed very well with the DFT calculated values (sign of the measured couplings was assumed to be the same as predicted by DFT calculations).

Scheme 2. Comparison of the Long-Range Correlations Observed in the 4 Hz Optimized HMBC Spectrum (panel A) and the 4 Hz (panel B) and 2 Hz (panel C) Optimized LR-HSQMBC Spectra of Cervinomycin A_2 (2)[a]

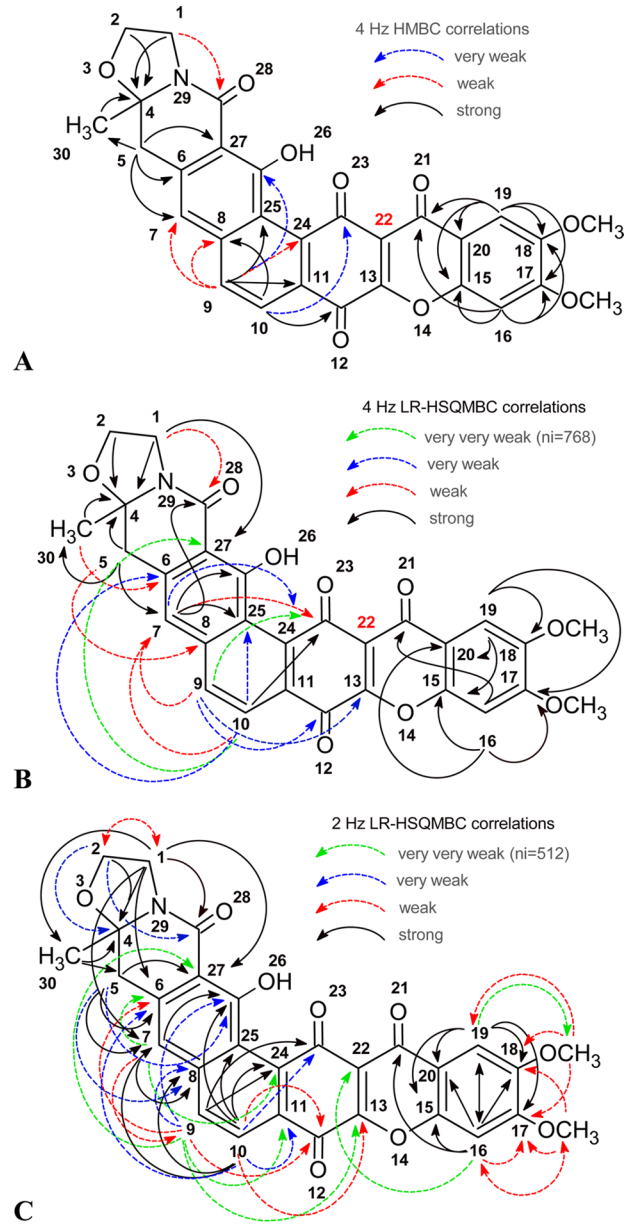

[a]The 4 Hz optimized HMBC spectrum afforded 8 $^4J_{CH}$ and 2 $^5J_{CH}$ correlations. In comparison, the 4 Hz optimized LR-HSQMBC spectrum afforded 9 $^4J_{CH}$ and 4 $^5J_{CH}$ correlations. Finally, the 2 Hz optimized LR-HSQMBC spectrum gave the greatest number of long-range correlations with 22 $^4J_{CH}$ correlations, 8 $^5J_{CH}$ correlations, and 1 $^6J_{CH}$ correlation. The 4 Hz optimized experiments were both acquired with 768 t_1 increments, whereas the 2 Hz optimized LR-HSQMBC spectrum was acquired with 512 t_1 increments. It should be noted that during the acquisition of the LR-HSQMBC spectra, that some of the weak correlations "grew in" with increasing numbers of t_1 increments acquired, with some only becoming visible when the acquisition was monitored at 384, 512, or even 640 t_1 increments completed. It is interesting to note that due to vanishingly small $^nJ_{CH}$ coupling constants, none of the 4 Hz experiments afforded any correlations that linked the H16 or H19 resonances to either the C13 or C22 resonances. A very very weak correlation from H16 to C22 was, however, observed in the 2 Hz optimized LR-HSQMBC data.

dx.doi.org/10.1021/jo500333u | J. Org. Chem. 2014, 79, 3887−3894

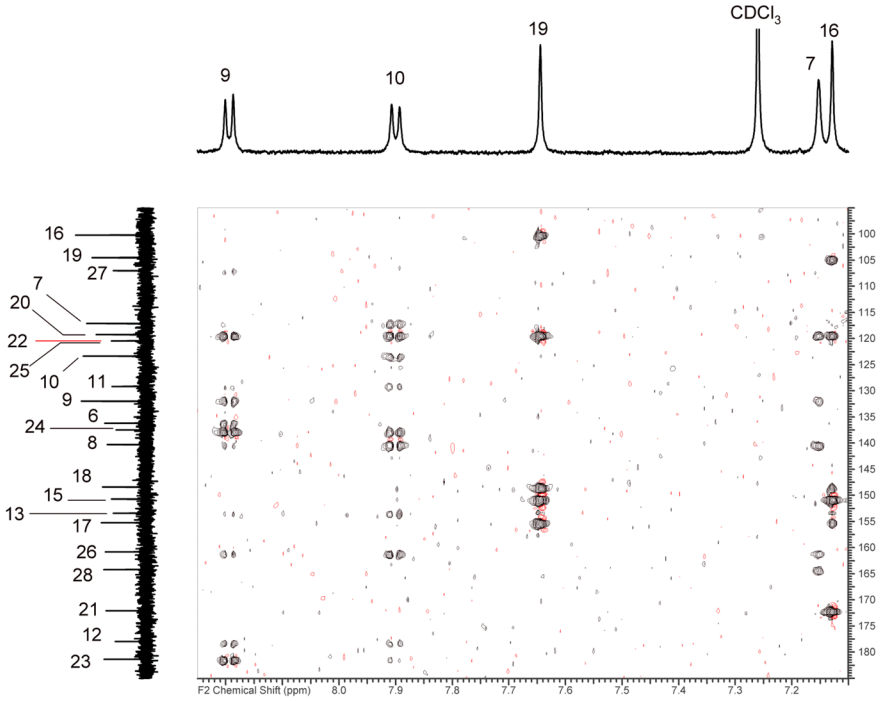

Figure 5. Expansion of the 2 Hz optimized LR-HSQMBC spectrum of a ~400 μg sample of cervinomycin A_2 (**2**) dissolved in 40 μL of deuterochloroform, which places ~250 μg in the *rf* coil of the probe. The data were acquired as 4096 × 512 points accumulating 32 transients/t_1 increment with a 1.5 s delay between transients giving an acquisition time of 21 h 30 m.

Most of the carbons in cervinomycin A_2 can be assigned on the basis of two- and three-bond J_{CH} correlations observed in the standard 8 Hz HMBC data. However, connecting the two quadrants of cervinomycin A_2 separated by the benzoquinone fragment is impossible on the basis of the two- and three-bond correlations from an HMBC spectrum and can only be done on the basis of long-range ($^4J_{CH}$) and very long-range ($^nJ_{CH}$, n = 5, 6) correlations. The LR-HSQMBC experiment allows detection of critical responses such as the 5-bond 0.78 Hz J_{CH} coupling between the H9 proton and the C13 carbon, which helps to unequivocally prove the earlier proposed structure (Scheme 2).

EXPERIMENTAL SECTION

The NMR data reported in this study were acquired using either a 4.9 mg sample of strychnine (**1**) (10.5 μmol) or a 400 μg sample of cervinomycin A_2 (**2**) (~0.75 μmol). Strychnine was obtained from Fluka under the Pestenal brand name, and the cervinomycin A_2 was obtained from Apollo Scientific, Stockport, Cheshire SK6 2QR, U.K. Each sample was dissolved in 40 μL of 99.96% $CDCl_3$ (Cambridge Isotope Laboratories, Andover, MA, USA) that was transferred to a 1.7 mm NMR tube (Bruker, Billerica, MA, USA) using a 24G flexible Teflon needle attached to a Hamilton gastight syringe.

All of the NMR data were acquired using a 600 MHz three-channel AVANCE III NMR spectrometer equipped with a gradient triple resonance TXI 1.7 mm TCI $^1H/^{13}C-^{15}N$ MicroCryoProbe. Data were accumulated with the sample temperature maintained at 30 °C.

The multiplicity-edited HSQC data on strychnine (**1**) were acquired as 2048 × 768 data points for the full spectrum accumulating 2 transients/t_1 increment, giving an acquisition time of 43 min. A squared sine-bell apodization phase-shifted 90° was applied prior to both Fourier transforms. Two $^1H-^{13}C$ HMBC spectra were acquired for strychnine one was optimized for 8 Hz and the other for 2 Hz. These data were acquired as 4096 × 512 points with 16 scans per each t_1 increment; the acquisition times were 2 h 11 min and 2 h 24 min, respectively. The HMBC spectra were linear predicted in F_1 to 1536 points and zero-filled to afford 4K × 2K spectra. Sine-bell apodization was applied prior to both Fourier transforms. The D-HMBC data were acquired and processed with parameters identical to the 2 Hz HMBC experiment. The LR-HSQMBC spectrum of strychnine was optimized for $^nJ_{CH}$ = 2 Hz. The comparative data were acquired as 4096 × 512 points with 8 transients accumulated per t_1 increment. The $^1J_{CH}$ delay was optimized for 145 Hz. A delay of 1.5 s was employed between transients, giving an overall acquisition time of 2 h 42 m. A squared sine-bell apodization phase-shifted 90° was applied prior to both Fourier transforms and these data were linear predicted to 768 points in F_1 and zero-filled to afford a 4K × 2K spectrum.

The inverted $^1J_{CC}$ 1,*n*-ADEQUATE spectra for strychnine were acquired using the dual optimized pulse sequence described by Reibarkh and co-workers.[9e] The experiment was optimized with $^1J_{CC}/^nJ_{CC}$ optimizations of 57/9.5 and 64/8 Hz as 3072 × 200 increments, with 64 transients/ t_1 increment giving an acquisition time of 24 h 22 min. These data were linear predicted to 400 points in F_1 and zero-filled to afford a 4K × 2K spectrum. Using these parameters, not all of the correlations were observed with sufficient digital resolution. The data were processed with linear prediction in the F_1 dimension and zero-filling to afford a final spectrum of 4K × 2K. All correlations were resolved. Furthermore, more $^nJ_{CC}$ correlations were observed in this spectrum than with the former parameters. A squared sine-bell apodization phase-shifted 90° was applied prior to both Fourier transforms for both experiments.

The multiplicity-edited HSQC data on cervinomycin A_2 (**2**) were acquired as 2048 × 200 data points for the full spectrum, giving an acquisition time of 45 min. A squared sine-bell apodization phase-shifted 90° was applied prior to both Fourier transforms. Two $^1H-^{13}C$ HMBC spectra were acquired for cervinomyin A_2, one was optimized for 8 Hz and the other for 4 Hz. These 8 Hz data were acquired in 1 h 38 m as 4096 × 384 points with 8 scans/t_1 increment; the 4 Hz data were acquired in 6 h 46 min as 4096 × 384 points with 32 scans/t_1 increment. The HMBC spectra were linear predicted in F_1 to 1536 points and zero-filled to afford 4K × 2K spectra. A sine-bell apodization was applied prior to both Fourier transforms.

The CLIP-HSQMBC experiments were acquired as a series of experiments with selective excitation applied at 8.18, 7.89, 7.67, 7.15, and 7.12 ppm with a 20 ms selective Gaussian π pulse. These data were acquired as 8192 × 96 points to afford 1.0 Hz resolution before

dx.doi.org/10.1021/jo500333u | J. Org. Chem. 2014, 79, 3887−3894

linear prediction and zero-filling. The data were processed using a squared sine-bell apodization phase-shifted 90° and applied prior to both Fourier transforms with linear prediction in the first frequency domain and zero-filling in the second to afford the final 16K × 1K spectrum. The experiments were optimized for 5 or 8 Hz and acquired with 32−64 scans per increment (see Supporting Information for additional details).

The LR-HSQMBC spectra acquired for cervinomycin A_2 employed a sample containing ∼400 μg of material in 40 μL of deuterochloroform, which gave ∼250 μg of material in the rf coil of the probe. The 4 Hz data were acquired as 4096 × 768 points, accumulating 16 transients/t_1 increment. The experiment was monitored by processing the data after 320, 512, and after the full acquisition of 768 points. Substantial signal was observed even in the final increment of the experiment. The data were acquired in 14 h 26 m and were processed using a squared sine-bell apodization phase-shifted 90° and applied prior to both Fourier transforms with linear prediction in the second frequency domain to 1536 points and zero-filling to afford the final 4K × 2K spectrum, a portion of which is shown in Figure 5. It should be noted that correlations "grow" in the 2D matrix as a function of increasing digital resolution in F_1 and it should not be assumed that a specific, small correlation not observed early in the course of the data acquisition will not be seen. Rather, weak correlations were observed to appear with increasing F_1 digital resolution. It should also be noted, that data containing all of the correlations summarized in Table 1 were acquired for this sample in as little as 2 h 42 m with excellent signal-to-noise (see Supporting Information). The 2 Hz LR-HSQMBC spectra was acquired as 4096 × 512 points, accumulating 32 transients/t_1 increment, which gave an acquisition time of 21 h 30 m. The experiment was monitored after the completion of 256 increments and again, still had strong signal in the last increment. The data were processed using a squared sine-bell apodization phase-shifted 90° and applied prior to both Fourier transforms with linear prediction in the second frequency domain to 1536 points and zero-filling to afford the final 4K × 2K spectrum.

■ ASSOCIATED CONTENT

Supporting Information

Bruker pulse program for LR-HSQMBC, comparison of in-phase vs antiphase peak amplitude and IP/AP peak ratios, table of calculated and experimental coupling constants for strychnine, table of LR-HSQMBC and 1,*n*-ADEQUATE data for strychnine, T_1 and T_2 relaxation data for strychnine, and supplementary LR-HSQMBC and CLIP-HSQMBC NMR data for strychnine and cervinomycin A_2. This material is available free of charge via the Internet at http://pubs.acs.org.

■ AUTHOR INFORMATION

Corresponding Author

*E-mail: robert.williamson2@merck.com.

Notes

The authors declare no competing financial interest.

■ ACKNOWLEDGMENTS

T.P. thanks MINECO (Spain) for funding (project CTQ2012-32436)

■ REFERENCES

(1) Breton, R. C.; Reynolds, W. F. *Nat. Prod. Rep.* **2013**, *30*, 501−524.
(2) Halabalaki, M.; Vougogiannopoulou, K.; Mikros, E.; Skaltsounis, A. L. *Curr. Opin. Biotechnol.* **2014**, *25*, 1−7.
(3) Martin, G. E.; Zektzer, A. S. *Magn. Reson. Chem.* **1988**, *26*, 631−652.
(4) Bax, A.; Summers, M. F. *J. Am. Chem. Soc.* **1986**, *108*, 2093−2094.
(5) (a) Reynolds, W. F. *Encycl. NMR Spectrosc.* **2011**, DOI: 10.1002/97804700334590.emrstm1176. (b) Schoefberger, W.; J. Schlagnitweit, J.; Mueller, N.; Webb, G. A. *Annu. Rep. NMR Spectrosc.* **2011**, *72*, 1−60. (c) Furrer, J.; Webb, G. A. *Annu. Rep. NMR Spectrosc.* **2011**, *74*, 294−354. (d) Furrer, J. *Concepts in Magn. Reson. A* **2012**, *40*, 101−127. (e) Furrer, J. *Concepts Magn. Reson., Part A* **2012**, *40*, 146−169.
(6) (a) Araya-Maturana, R.; Delgado-Castro, T.; Cardona, W.; Weiss-López, B. E. *Curr. Org. Chem.* **2001**, *5*, 253−263. (b) Araya-Maturana, R.; Pessoa-Mahana, H.; Weiss-López, B. *Nat. Prod. Commun.* **2008**, *3*, 445−450.
(7) (a) Krishnamurthy, V. V.; Russell, D. J.; Hadden, C. E.; Martin, G. E. *J. Magn. Reson.* **2000**, *146*, 232−239. (b) Hadden, C. E.; Martin, G. E.; Krishnamurthy, V. V. *Magn. Reson. Chem.* **2000**, *38*, 143−147.
(8) (a) Nyberg, N. T.; Duus, J. Ø.; Sørensen, O. W. *J. Am. Chem. Soc.* **2005**, *127*, 6154−6155. (b) Nyberg, N. T.; Duus, J. Ø.; Sørensen, O. W. *Magn. Reson. Chem.* **2005**, *43*, 971−974. (c) Benie, A. J.; Sørensen, O. W. *J. Magn. Reson.* **2007**, *184*, 315−321. (d) Petersen, B. O.; Vinogradov, E.; Kay, W.; Würtz, P.; Nyberg, N. T.; Duus, J. Ø.; Sørensen, O. W. *Carbohydr. Res.* **2006**, *341*, 550−556.
(9) (a) Martin, G. E.; Webb, G. A. *Annu. Rep. NMR Spectrosc.* **2011**, *74*, 215−291. (b) Martin, G. E.; Hilton, B. D.; Blinov, K. A. *J. Nat. Prod.* **2011**, *74*, 2400−2407. (c) Martin, G. E.; Williamson, R. T.; Dormer, P. G.; Bermel, W. *Magn. Reson. Chem.* **2012**, *50*, 563−568. (d) Martin, G. E.; Blinov, K. A.; Reibarkh, M.; Williamson, R. T. *Magn. Reson. Chem.* **2012**, *50*, 722−728. (e) Reibarkh, M.; Williamson, R. T.; Martin, G. E.; Bermel, W. *J. Magn. Reson.* **2013**, *236*, 126−133. (f) Martin, G. E.; Buevich, A. V.; Reibarkh, M.; Singh, S.; Ondyka, J. G.; Williamson, R. T. *Magn. Reson. Chem.* **2013**, *51*, 383−389. (g) Senior, M. M.; Williamson, R. T.; Martin, G. E. *J. Nat. Prod.* **2013**, 2088−2093.
(10) (a) Williamson, R. T.; Márquez, B. L.; Gerwick, W. H.; Kövér, K. E. *Magn. Reson. Chem.* **2000**, *38*, 265−273. (b) Williamson, R. T.; Boulanger, A.; Vulpanovici, A.; Roberts, M. A.; Gerwick, W. H. *J. .Org. Chem.* **2002**, *67*, 7927−7936.
(11) Furihata, K.; Seto, H. *Tetrahedron Lett.* **1995**, *36*, 2817−2820.
(12) (a) Saurí, J.; Parella, T.; Espinosa, J. F. *Org. Biomol. Chem.* **2013**, *11*, 4473−4478. (b) Krishnamurthy, V. V. *J. Magn. Res., Ser. A* **1996**, *121*, 33−41.
(13) Enthart, A.; Freudenberger, J. C.; Furrer, J.; Kessler, H.; Luy, B. J. *Magn. Reson.* **2008**, *192*, 314−322.
(14) (a) Berger, S.; Braun, S. *200 and More NMR Experiments*; Wiley: New York, 2004. (b) Parella, T.; Espinosa, J. F. *Prog. Nucl. Magn. Reson. Spectrosc.* **2013**, *73*, 17−55. (c) Márquez, B. L.; Gerwick, W. H.; Williamson, R. T. *Magn. Reson. Chem.* **2001**, *39*, 499−530.
(15) (a) Gil, S.; Espinosa, J. F.; Parella, T. *J. Magn. Reson.* **2010**, *207*, 312−321. (b) Nolis, P.; Espinosa, J. F.; Parella, T. *J. Magn. Reson.* **2006**, *179*, 295−306.
(16) (a) Williamson, R. T.; Buevich, A. V.; Martin, G. E. *Org. Lett.* **2012**, *14*, 5098−5101. (b) Bifulco, G.; Riccio, R.; Martin, G. E.; Buevich, A. V.; Williamson, R. T. *Org. Lett.* **2013**, *15*, 654−657. (c) Butts, C. P.; Jones, C. R.; Harvey, J. N. *Chem. Commun.* **2011**, *47*, 1193−1195.
(17) Deng, W.; Cheeseman, J. R.; Frisch, M. J. *J. Chem. Theory and Comput.* **2006**, *2*, 1028−1037.
(18) Ōmura, S.; Iwai, Y.; Hinotozawa, K.; Takahashi, Y.; Kato, J.; Nakagawa, A.; Hirano, A.; Shimizu, H.; Haneda, K. *J. Antibiot.* **1982**, *35*, 645−652.
(19) (a) Ralifo, P.; Crews, P. *J. Org. Chem.* **2004**, *69*, 9025−9029. (b) Molinski, T. F.; Morinaka, B. I. *Tetrahedron* **2012**, *68*, 9307−9343.
(20) Nakagawa, A.; Omura, S.; Kushida, K.; Shimizu, H.; Lukacs, G. *J. Antibiot.* **1987**, *3*, 301−308.
(21) R. Freeman, R.; Morris, G. A. *J. Chem. Soc., Chem. Commun.* **1978**, 684−686.
(22) Seto, H.; Sasaki, T.; Yonehara, H.; Uzawa, J. *Tetrahedron Lett.* **1978**, 923−926.
(23) Drautz, H.; Keller-Schierlein, W.; Zahner, H. *Arch. Microbiol.* **1975**, *106*, 175−190.
(24) (a) Gurevich, A. I.; Karapetyan, M. N.; Kolosov, V. N.; Omelchenko, V. V.; Onoprienko, G. I. *Tetrahedron Lett.* **1972**, *13*,

1751−1754. (b) Liu, W. C.; Cullen, W. P.; Rao, K. V. *Antimicrob. Agents Chemother.* **1962**, *1963*, 767−771.
(25) Lee, T. M.; Borders, D. B.; Carter, G. T.; Hertz, M.; Kirby, J. P. *Program and Abstracts of the 26th Interscience Conference on Antimicrobial Agents and Chemotherapy, New Orleans, Sept 28−Oct 1, 1986*; American Society for Microbiology: Washington, DC, 1986No. 222, p 136,.
(26) Saurí, J.; Parella, T.; Espinosa, J. F. *Org. Biomol. Chem.* **2013**, *11*, 4473−4478.

■ NOTE ADDED AFTER ASAP PUBLICATION

This paper was published ASAP on April 18, 2014. Figure 1 was updated. The revised paper was reposted on May 2, 2014.